Dalton Transactions

Accepted Manuscript

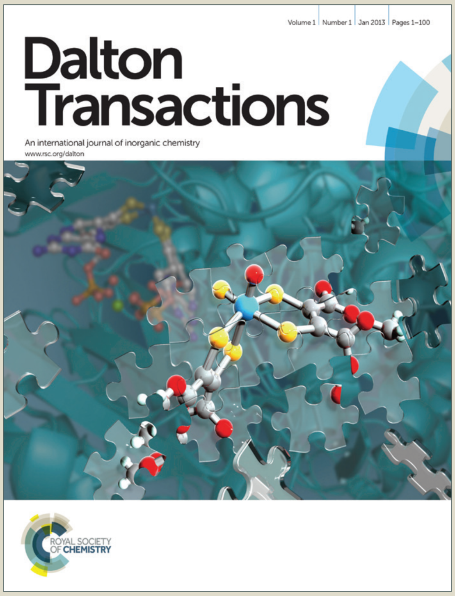

ROYAL SOCIETY OF CHEMISTRY

www.rsc.org/dalton

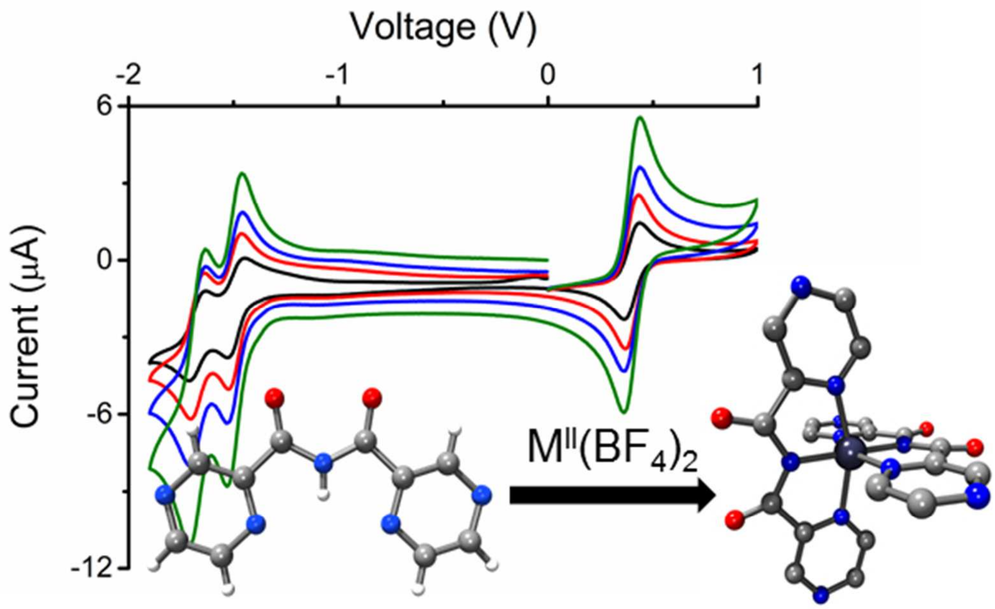

159x100mm (96 x 96 DPI)

Cite this: DOI: 10.1039/c0xx00000x

www.rsc.org/xxxxxx

ARTICLE TYPE

Pyrazine-imide complexes: reversible redox and MOF building blocks

Matthew G. Cowan, Reece G. Miller and Sally Brooker*

Received (in XXX, XXX) Xth XXXXXXXXX 20XX, Accepted Xth XXXXXXXXX 20XX
DOI: 10.1039/b000000x

The synthesis of the symmetric pyrazine imide ligand, *N*-(2-pyrazylcarbonyl)-2-pyrazinecarboxamide, (Hdpzca) and five new first row transition metal complexes of it are reported: $[M^{II}(dpzca)_2]$, M^{II} = Fe, Cu, Zn; $\{[Cu^{II}(dpzca)(H_2O)_n]_{1\text{ or }2}X\}$, X = BF_4^- or SiF_6^{2-}, n = 2 or 3. The crystal structures of Hdpzca, $[Co^{II}(dpzca)_2]$, $[Cu^{II}(dpzca)_2]$, $\{[Co^{III}(dpzca)_2](BF_4)\}_2\cdot 5CH_3CN$ and $[Cu^{II}(dpzca)(H_2O)_3]_2SiF_6\cdot 2H_2O$ were determined and reveal an orthogonal positioning of the 'spare' pyrazine nitrogen atoms and 'spare' pairs of imide oxygen atoms. The $[M^{II}(dpzca)_2]$ complexes are therefore useful six-coordinate building blocks for producing larger supramolecular assemblies. Two examples of secondary assembly of $[M^{II}(dpzca)_2]$ complexes, with M = Co and Ni, with silver nitrate gave single crystals: $\{[Co^{III}(dpzca)_2Ag](NO_3)_2\cdot 2H_2O\}_n$ and $\{([Ni^{II}(dpzca)_2Ag^{I}{}_{½}](½NO_3)(xH_2O\}_n$ were structurally characterised . The redox processes of $[M^{II}(dpzca)_2]$, with M^{II} = Fe, Ni, Cu and Zn, are reported and, as seen for M^{II} = Co, reversible metal- and ligand-based redox processes are observed, with $E_m(M^{II}/M^{III})$ values 0.15-0.24 V higher than for the analogous complexes of Hpypzca (non-symmetric pyridine/pyrazine imide ligand), and 0.35-0.36 V higher than for the complexes of Hbpca (symmetric pyridine imide ligand).

Introduction

Imides are a relatively under-exploited ligand class, with only 12 imide ligands and 150 structurally characterised imide complexes reported by mid-2011.[1] The first structurally characterised imide complex was reported in 1976, with the imide formed accidentally, by hydrolysis of the initial triazine ligand.[2, 3] By far the most commonly employed imide is the symmetric pyridine based ligand Hbpca (Fig. 1). Deprotonation of such imide ligands results in a mono-anionic N_3-donor ligand and the formation of a wide variety of complexes. The mononuclear $[M(bpca)Y_n]^{x+}$ and $[M(bpca)_2]^{x+}$ complexes have a pair or two pairs, respectively, of 'spare' imide oxygen atoms which are available for secondary coordination to additional metal ions (transition metal or lanthanide ions). Hence they have been used as building blocks to generate a large number of discrete and polymeric structural motifs.[1] The resulting 1-, 2- and 3-D assemblies are frequently mixed-valent or mixed-metal complexes, and have displayed a range of interesting properties including Single Molecule Magnetism (SMM),[4, 5] Single Chain Magnetism (SCM)[6, 7] or luminescence,[8] as well as generating anion-exchangeable[9] or CO_2 vs N_2 selective[10] Metal Organic Frameworks (MOFs).

We have previously reported the synthesis, structures and redox properties of a family of transition metal complexes of a new, non-symmetric pyrazine/pyridine analogue, Hpypzca, of the symmetric pyridine based imide ligand Hbpca (Fig. 1 & 2).[11] Consistent with replacing one pyridine ring by a pyrazine ring in each ligand, the $[M^{II}(pypzca)_2]$ complexes with M = Ni, Co, Fe undergo reversible redox, M^{II} ↔ M^{III}, at higher potentials than observed for the analogous Hbpca complexes. We also noted that the 'spare' pyrazine nitrogen atoms add another pair of potential secondary coordination sites to these complexes, forming a 'corner' type building block, that the usual secondary coordination through the pairs of 'spare' imide oxygen atoms can extend along a third axis (Fig. 2, top right).

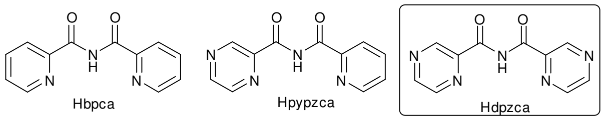

Fig. 1 The most studied imide ligand to date, Hbpca, and two new imide ligands, Hpypzca and Hdpzca, developed in this group.

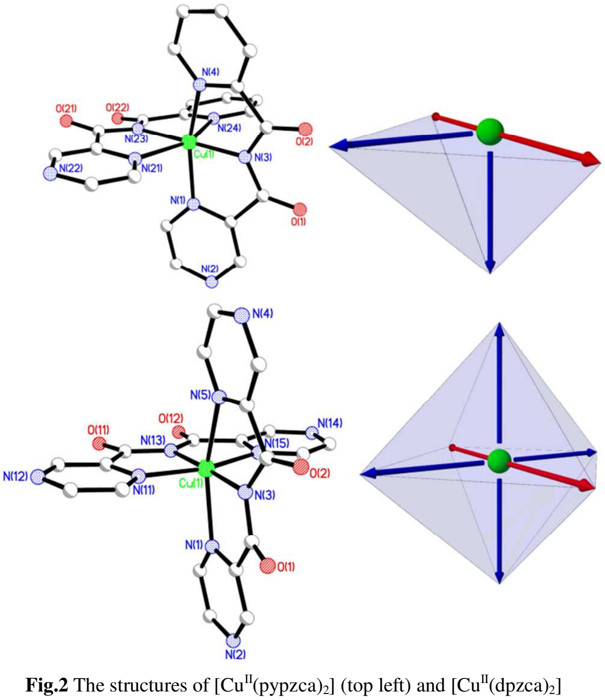

Fig.2 The structures of $[Cu^{II}(pypzca)_2]$ (top left) and $[Cu^{II}(dpzca)_2]$ (bottom left). These complexes can be thought of as 'building blocks' (right). The 'all pyrazine complex' building block is reminiscent of an octahedron, with the 'spare' pyrazine nitrogen atoms (blue arrows) the four imide oxygen atoms (red arrows) positioned orthogonally.

More recently, we have developed access to a new symmetric pyrazine based ligand Hdpzca (Fig. 1), in which both of the pyridine rings are replaced by pyrazine rings. The resulting mononuclear $[Co^{II}(dpzca)_2]$ complex was shown to be triply switchable, undergoing temperature or pressure induced spin crossover as well as reversible $Co^{II} \leftrightarrow Co^{III}$ redox.[12, 13] In addition, the cobalt and nickel $[M^{II/III}(dpzca)_2]$ building block complexes (Figure 2 bottom; M = Co^{II}, Co^{III} and Ni^{II}) were used, via secondary coordination to Ag^I ions (i.e. as secondary building units, SBUs[14]), to generate two coordination polymers, or MOFs, $[Co^{III}(dpzca)_2Ag](BF_4)_2$ (**1**) and $[Ni^{II}(dpzca)_2Ag]BF_4$ (**2**).[10] These MOFs are robust and isostructural, but due to the different oxidation states they differ in the number of anions in the channels. Both selectively absorb CO_2 over N_2, albeit with a low CO_2 capacity. Interestingly **1** is more selective than **2**, perhaps due to the greater anion content of the channels.[10]

Here we detail the synthesis of the Hdpzca ligand, as well as the preparation, structures, magnetic and electrochemical properties of a series of mononuclear transition metal building block complexes from it, and the synthesis and structures of two coordination polymers by reaction of two of these SBUs with silver(I) nitrate (Fig. 2 and 3).

Results and Discussion

Ligand Synthesis

The synthetic method used to produce Hpypzca and other imide ligands[8, 11, 15] was adapted for the preparation of the new imide ligand Hdpzca. Accordingly, in the first step, 2-pyrazinecarbonyl chloride was prepared from commercially available 2-pyrazinecarboxylic acid using $SOCl_2$. In our hands, the distillation methods reported in the literature[16] failed to reproducibly purify the acid chloride from the dark purple by-product (which the literature for the pyridine analogue[17] indicates is the product of self-condensation of the acid chloride to form a dihydropyrazine-pyrazinium salt). Hence we instead used the crude, purple, acid chloride sample without further purification in the next step, reaction with commercially available 2-pyrazinecarboxamide to form the imide ligand (Fig. 3). More of the dark purple contaminant was formed during the reaction to form the imide, but it did not appear to interfere with the reaction or to react with the amide to generate additional by-products. Rather, the desired ligand, Hdpzca, was obtained.

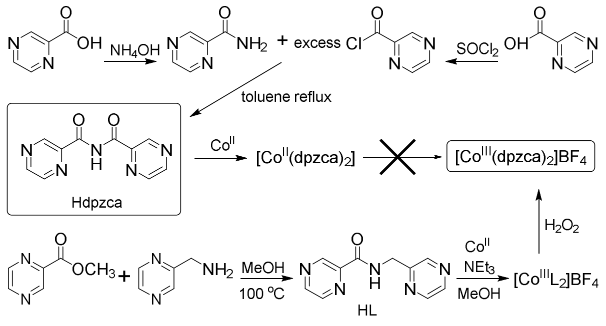

Fig. 3 The preparation of the new symmetric pyrazine imide ligand Hdpzca, and a summary of the two synthetic routes explored for the preparation of $[Co^{III}(dpzca)_2]BF_4$.

The best yield of Hdpzca was obtained by refluxing a 40% excess of the crude acid chloride with the amide in dry toluene for three days (Fig. 3). For two reasons, an additional 0.85 equivalents of the acid chloride were then added to ensure that none of the amide starting material remained. Firstly, the excess is necessary as the acid chloride decomposes during the reaction, and secondly the amide proved to be difficult to separate from the imide ligand. Once thin layer chromatography of the reaction solution (using 1:1 dichloromethane/acetone) showed that no amide reagent remained, methanol was added to the reaction solution to convert any remaining acid chloride reagent to the corresponding ester, thereby making it trivial to separate from the imide ligand. The solution was evaporated to dryness under reduced pressure, the resulting solid suspended in dichloromethane and filtered through a celite plug. This removed the purple by-product as it adheres to the celite (N.B. silica gel does not work). The dichloromethane filtrate was taken to dryness, acetone added and the resulting suspension sonicated before filtration to give clean Hdpzca in good yield (77%). The excess ester could then be recovered from the acetone solution. Single crystals of Hdpzca suitable for structural characterisation were obtained by vapour diffusion of diethylether into a dichloromethane solution.

Synthesis of $[M^{II}(dpzca)_2]$ complexes

As for the synthesis of $[Co^{II}(dpzca)_2]$ (red, 87%) and $[Ni^{II}(dpzca)_2]$ (tan, 85%),[10, 12] the complexes $[Fe^{II}(dpzca)_2]$ (purple, 94%), $[Cu^{II}(dpzca)_2]$ (green, 84%) and $[Zn^{II}(dpzca)_2]$ (white, 44%) were prepared by combining a methanol or acetone solution of the hydrated tetrafluoroborate metal salt and a dichloromethane solution containing two equivalents of both Hdpzca and triethylamine. The desired complexes immediately precipitated and the resulting powders were isolated by filtration before drying in vacuo.

At room temperature these $[M^{II}(dpzca)_2]$ complexes are insoluble in most common solvents and have very low solubility in others (Tables S1-S5) which hindered attempts to generate crystalline samples by recrystallisation. Instead, crystalline samples of all of the complexes, except that of copper(II), were obtained by carrying out the reactions by the slow diffusion of triethylamine into a well-mixed methanol/dichloromethane solution of the metal salt and ligand. In contrast, mixing the copper(II) salt and Hdpzca caused immediate precipitation of $[Cu^{II}(dpzca)_2]$ as a powder, without addition of base. That the reaction with copper(II) does not require a base is unsurprising given its well established ability to compete for nitrogen atom donors with protons.[18]

Of the crystals grown using this slow diffusion of triethylamine method, only those of $[Co^{II}(dpzca)_2]$ were suitable for structural characterisation.[12] Crystals of $[Cu^{II}(dpzca)_2]$ suitable for structural characterisation were grown from slow evaporation of a small amount of dilute chloroform solution.

Synthesis of $[M^{III}(dpzca)_2]X$ complexes

The mild oxidative conditions used to prepare $[Co^{III}(pypzca)_2]BF_4$ (addition of water to the reaction suspension)[11] did not work for the synthesis of $[Co^{III}(dpzca)_2]BF_4$, probably due to the very low solubility of $[Co^{II}(dpzca)_2]$. This also prevented facile chemical oxidation of $[Co^{II}(dpzca)_2]$ by the stronger oxidant hydrogen peroxide (Fig. 3). Instead a synthetic route from the analogous amide ligand, (2-pyridylmethyl)-2-pyridinecarboxamide, HL (Fig. 3), was developed and optimised,[10] based on observations from the investigations of related amide based ligands which show facile oxidation of methylene links in amides to imides in the presence of transition metal ions.[1, 19-21]

The methylene-linked amide ligand, HL, was prepared, then combined with triethylamine and $[Co^{II}(H_2O)_6](BF_4)_2$ in methanol (N.B. this does not work in acetonitrile), and treated with 5.5 equivalents of hydrogen peroxide (Fig. 3). The crude $[Co^{III}(dpzca)_2]BF_4$ gradually precipitated and was isolated by filtration, then washed with a large amount of methanol to remove the excess and protonated triethylamine (traces readily observed by mass spectrometry) and recrystallised from an approximately 9:1 acetonitrile/water mixture. In practice this was done by suspending approximately 100 mg of material in 15 mL of boiling acetonitrile and adding water until the suspension became a solution. Crystals would not grow when the procedure was attempted in methanol or in water. Furthermore, the scale of the recrystallisation was unable to be successfully increased beyond 150 mg. Crystals of $\{[Co^{III}(dpzca)_2]BF_4\}_2 \cdot 5CH_3CN$ were prepared on one occasion by vapour diffusion of diethylether into an acetonitrile solution of $[Co^{II}(dpzca)_2](BF_4)$ and silver tetrafluoroborate. This method could not be used for purification purposes as it does not separate $\{[Co^{III}(dpzca)_2](BF_4)\}_2 \cdot 5MeCN$ from contaminants including unoxidised $[Co^{II}(dpzca)_2]$ and Ag^{o}. As reported for the series of complexes generated with Hpypzca,[11] the carbonyl stretch of $[Co^{III}(dpzca)_2]BF_4$ (1719 cm^{-1}) is considerably higher in energy than that of the $[M^{II}(dpzca)_2]$ complexes (1692-1701 cm^{-1}). The stretch is similar to those of the $[M^{III}(pypzca)_2]BF_4$ (M^{III} = Fe, Co) complexes (1719-1722 cm^{-1}).[11]

Synthesis of $[Cu^{II}(dpzca)(H_2O)_n]X$ complexes

The preparation of $[Cu^{II}(dpzca)(H_2O)_2]BF_4 \cdot H_2O$ was attempted in order to examine the expected differences in secondary interactions between $[Cu^{II}(dpzca)(H_2O)_2]BF_4 \cdot H_2O$ and its non-symmetric ligand analogue $[Cu^{II}(pypzca)(H_2O)_2]BF_4 \cdot H_2O$.[11] Initially the same reaction protocol used for $[Cu^{II}(pypzca)(H_2O)_2]BF_4 \cdot H_2O$ was followed. A 1:1 mixture of copper(II) and Hdpzca was combined in a methanol/dichloromethane solution, followed by the addition of water and slow evaporation. The blue-green crystals obtained in this manner were used for X-ray structure determination, however they were found to be of very low quality and the resulting structure of $[Cu^{II}(dpzca)(H_2O)_2]BF_4 \cdot H_2O$ was incomplete so is not presented here. During attempts to recrystallise the sample from boiling water a slight colour change to a darker green was observed. Structural characterisation of the resulting crystals showed that the tetrafluoroborate anions had presumably reacted with silicon dioxide from the glassware, as they had formed hexafluorosilicate anions, producing crystals of the complex $[Cu^{II}(dpzca)(H_2O)_3]_2SiF_6 \cdot 2H_2O$ in 29% yield. This synthesis was reproducible. The efficient production of SiF_6^{2-} anions has been reported previously, including for copper(II) complexes of the related amide ligand H_2L^{S1}.[22]

Crystal structures

Hdpzca, $[Co^{II}(dpzca)_2]$,[12] $\{[Co^{III}(dpzca)_2]BF_4\}_2 \cdot 5CH_3CN$, $[Cu^{II}(dpzca)_2]$, and $[Cu^{II}(dpzca)(H_2O)_3]_2SiF_6 \cdot 2H_2O$ have been structurally characterised (Fig. 2, 4-6, S1 and Tables 1 and S6-S8). The structural characteristics of the high and low spin forms of $[Co^{II}(dpzca)_2]$ are discussed in detail in our previous paper.[12]

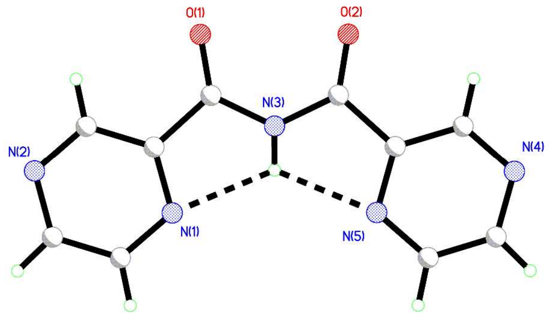

Fig.4 The structure of metal-free ligand Hdpzca. Note the planarity of the entire ligand.

The structure of metal-free Hdpzca is planar (Fig. 4): the largest deviation from the plane of all non-hydrogen atoms is the imide nitrogen atom [-0.069(3) Å]. This feature is similar to the symmetric quinoline based ligand Hbqca[23] but not to the pyridine/imide oligomers which adopt a helical structure.[15] The remarkable planarity is the result of Hdpzca being fully conjugated and the bifurcated *intra*-molecular hydrogen bonding between the imide hydrogen atom H(3)X and the pyrazine nitrogen atoms N(1) and N(5) [N(3)···N(1) 2.636(4), N(3)···H(3)X···N(1) 111.9°; N(3)···N(5) 2.631(4), N(3)···H(3)X···N(5) 111.9°]. The ^{1}H-NMR signal for H(3)X is at 12.42 ppm in d_6-DMSO, comparable to those observed for pyridine/imide oligomers (12.96 ppm $CDCl_3$, 12.66 ppm in d_6-DMSO) which are also stabilised by *intra*-molecular hydrogen bonds in the solid state.[15] Importantly the imide hydrogen signal has been reported at 10.28 ($CDCl_3$) and 11.53 ppm (d_6-DMSO) for imide molecules that cannot undergo similar *intra*-molecular hydrogen bonding.[24] Unfortunately these molecules have not been structurally characterised, preventing a detailed structural comparison.

For the complexes of Hdpzca we observe that the ligand is deprotonated and coordinated via the N_3 donor set (Fig. 2, 5, 6, S1), in an identical fashion to the analogues Hbpca and Hpypzca.[1, 11] For Hdpzca this leaves two sets of imide oxygen atoms and *four* 'spare' pyrazine nitrogen donors available for secondary coordination.[10] The octahedral orientation of these 'sets' of assembly instructions is summarised in Table 1 and illustrated in Figure 2.

The general structural features of these four complexes are similar to those summarised for the analogous complexes of Hpypzca.[11] In $\{[Co^{III}(dpzca)_2]BF_4\}_2 \cdot 5CH_3CN$, and $[Cu^{II}(dpzca)_2]$, two meridionally coordinated dpzca anions are bound to the metal ion at almost right angles to one another, providing an approximately octahedral coordination geometry (Fig. 2, 6 and S1, Table 1). As anticipated from previous studies, all of the M-N bond lengths are shorter for cobalt(III) than for the divalent transition metal ions. The copper(II) ion of $[Cu^{II}(dpzca)_2]$ is slightly more Jahn-Teller distorted than the copper(II) ion of $[Cu^{II}(pypzca)_2]$ (T = 0.87 and 0.90 respectively).[11]

Table 1 Selected bond lengths (Å), angles (°) and other parameters for the structurally characterised monometallic $[M(dpzca)_2]^{0/+}$ complexes.

Parameter	**$[Co^{II}(dpzca)_2]^{d,\ 12}$**	**$[Co^{III}(dpzca)_2]BF_4{\cdot}5CH_3CN$**	**$[Cu^{II}(dpzca)_2]$**
Temperature (K)	298	93	90
M-N_{pz}	2.145(3)	1.929(4), 1.925(4) 1.931(4), 1.930(4)	2.306(2), 2.320(2) 2.063(2), 2.059(2)
M-N_{imide}	2.049(4)	1.882(4), 1.894(4)	1.993(2), 1.955(2)
N_{pz}-M-N_{imide}	77.51(7)	83.8(2), 83.6(2) 84.3(2), 83.0(2)	78.18(8), 77.25(8) 81.24(8), 80.86(2)
N_{pz}-M-N_{pz}	102.49(7)	167.4(2), 167.4(2)	155.43(7), 161.91(8)
O_{imide} out of N_3 plane[a]	O(1) -0.376 O(1A) 0.376	-0.15(1); 0.25(1) 0.105(9); -0.100(8)	O(1) 0.167(7) O(2) -0.169(7) O(21) 0.307(7) O(22) -0.387(7)
Intra-ligand centroid$_{OO}$[b]···M···$N_{pz'}$[c]	73.3	78.7, 79.2 79.6, 79.3	70.7, 70.9 76.0, 76.3
Inter-ligand centroid$_{OO}$[b]···M···$N_{pz'}$[c]	106.7	100, 100 101, 100	102, 106 105, 113
Intra-ligand $N_{pz'}$···M···$N_{pz'}$	155.0(1)	158.79(7) 157.92(9)	141.60(4) 152.07(4)
Inter-ligand $N_{pz'}$···M···$N_{pz'}$	94.73(3)	95.69(8), 88.53(8) 90.92(8), 92.88(8)	90.22(4), 97.34(4) 93.50(4), 97.12(4)
Distortion parameter[e]	Σ = 110.6	Σ = 54.6	Σ = 83.7, T = 0.87

[a] The plane is defined by the coordinated N_3 donor set of the same ligand; [b] centroid of the oxygen imide atoms; [c] pz and pz' refer to the coordinated and 'spare' pyrazine donors respectively; [d] Note all pyrazine rings are equivalent due to crystallographic symmetry; [e] Distortion parameters were calculated as described in the following references T,[25] Σ.[26]

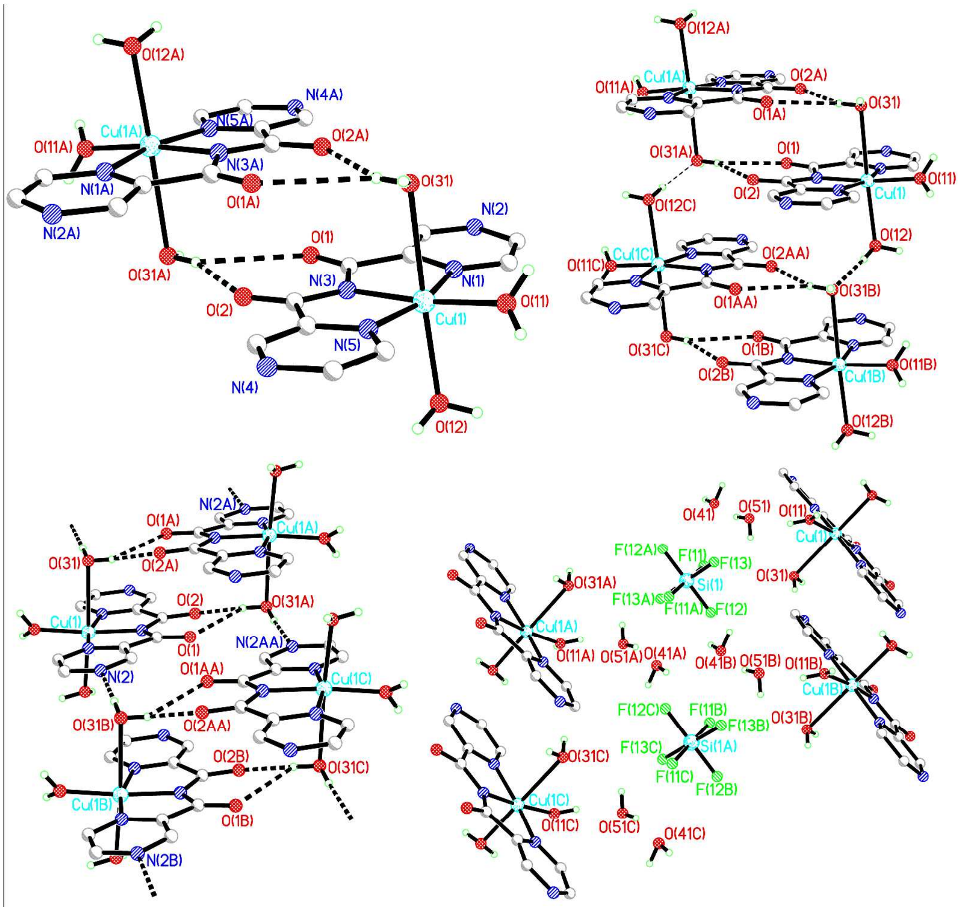

Fig. 5 The packing of $[Cu^{II}(dpzca)(H_2O)_3]_2SiF_6{\cdot}2H_2O$. The complex forms dimers (top left, A = 1-x, 1-y, 2-z). These dimers are assembled through hydrogen bonding interactions into double stranded chains (top right (B = x+1, y, z) and bottom left (B = x, y-1, z)). These stacks are separated by layers of SiF_6^{2-} counterions and water molecules (bottom right A = -x, 2-y, 1-z)). Note that non-acidic hydrogen atoms, solvent molecules and anions have been excluded for clarity where appropriate.

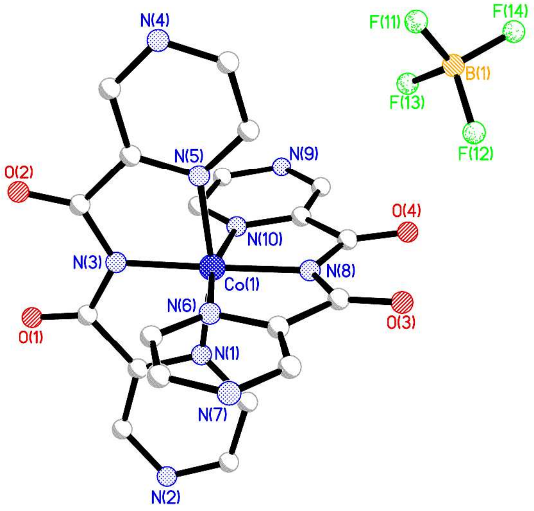

Fig. 6 The structure of {[Co^{III}(dpzca)$_2$](BF$_4$)}$_2$·5CH$_3$CN (H atoms, solvent molecules and a second cation/anion pair in the asymmetric unit have been excluded for clarity.

The secondary coordination sites in the [M$^{II/III}$(dpzca)$_2$]$^{0/+}$ units are arranged in an approximately octahedral fashion (Fig. 2, Table 1). This makes the complexes useful as SBUs, for example in the construction of MOFs,[27, 28] as we recently demonstrated for the M = Co^{III} and Ni^{II} complexes using a silver(I) connector, with the resulting pair of robust isomorphous MOFs, **1** and **2**, capable of selective gas uptake.[10] Similar to the complexes of Hpypzca the angles between the 'spare' pyrazine nitrogen atoms on separate ligands are approximately orthogonal (88.53-97.34°). However the angle between 'spare' pyrazine donors within the same ligand varies between 141.60 and 158.79°, quite distorted from the 'ideal' 180°. Similarly the angles between the centroid of the imide oxygen atoms and the spare pyrazine nitrogen atoms is distorted away from the orthogonal ideal for both for *intra*- (70.7-79.6°) and *inter*-ligand (100.4-113.2°) cases.

Similar to the copper(II) complex of the non-symmetric (pyridine/pyrazine imide) ligand, [Cu^{II}(pypzca)(H$_2$O)$_2$]BF$_4$·H$_2$O, that of the symmetric (all pyrazine imide) ligand, [Cu^{II}(dpzca)(H$_2$O)$_3$]$_2$SiF$_6$·2H$_2$O, features a large number of strong hydrogen bonding interactions (Fig. 5). The [Cu^{II}(dpzca)(H$_2$O)$_3$]$^+$ units are linked together into dimers through uneven 'two acceptor' bifurcated hydrogen bonds to the axially coordinated water molecule [O(31)] [O(31)-H···O(1A)/O(2A) 3.387, 2.782 Å; 125.60, 160.25°]. The dimers are stacked into double stranded chains by O(31) accepting a hydrogen bond from the other axially coordinated water molecule [O(12)] on an adjacent water molecule [O(12)-H···O(31B) 2.857 Å; 176°]. These chains are connected in the second dimension by O(31) hydrogen bonding to a 'spare' pyrazine nitrogen atom on an neighbouring complex [H-O31···N2 2.937 Å, 170°]. These chains are separated by layers of hexafluorosilicate anions and solvent water molecules. A hydrogen bond network is formed between the solvent water molecules and anions [O(51)-H···O(41) 2.935 Å, 163°; [O(41A)-H···F(11B) 3.151 Å, 119°; O(41A)-H···F(12C) 2.708 Å, 143°; O(51)-H···F(11) 2.877 Å, 109°; O(51)-H···F(13) 2.901 Å, 123°]. A connection between the chains of complexes and the anion/solvent layers occurs through hydrogen bonds between two of the three coordinated water molecules and the uncoordinated water molecules of solvation [O(51)-H···O(11) 2.627 Å, 158°; O(12)-H···O(41) 2.782 Å, 166°].

Electrochemical studies

Despite the low solubility of the [M^{II}(dpzca)$_2$] complexes in acetonitrile, the electrochemical processes could be observed (Table 1), either by using solutions of < 1 mmolL^{-1} complex and/or by studying a suspension. As for the pypzca complexes,[11] the magnitude of the current signal was increased by using bulk electrolysis of the suspension to provide the more soluble [M^{III}(dpzca)$_2$]$^+$ form in situ (Fig. 7 & 8). The quasi-reversible oxidation of [Ni^{II}(dpzca)$_2$] ↔ [Ni^{III}(dpzca)$_2$]$^+$ was accompanied by a significant colour change from an almost colourless suspension to a dark green solution (Fig. S11). Likewise the reversible oxidation of [Fe^{II}(dpzca)$_2$] ↔ [Fe^{III}(dpzca)$_2$]$^+$ was accompanied by a significant colour change from a dark purple suspension to an orange solution (Fig. 7). The bulk electrolysis carried out on this compound (Fig. S5 and S6) required significantly longer (15000 vs. 4000 seconds) than that on [Ni^{II}(dpzca)$_2$], as [Fe^{II}(dpzca)$_2$] is much less soluble, indeed is almost completely insoluble, in acetonitrile.

The *reversible* ligand-based electrochemical processes of the complexes [Co^{II}(dpzca)$_2$],[12] [Fe^{II}(dpzca)$_2$], [Ni^{II}(dpzca)$_2$] and [Zn^{II}(dpzca)$_2$] (Fig. 8, S4-S16, Table 2) are similar to those reported for [M$^{II/III}$(bpca)$_2$]$^{0/+}$ and [M$^{II/III}$(pypzca)$_2$]$^{0/+}$ (Tables 3, 4). However, the M^{II} ↔ M^{III} processes occur 0.15-0.24 V higher than those of the pyrazine-pyridine imide complexes, [M$^{II/III}$(pypzca)$_2$]$^{0/+}$, and in turn these occur at 0.11-0.20 V higher than for the pyridine-pyridine imide complexes, [M$^{II/III}$(bpca)$_2$]$^{0/+}$, indicating that the dpzca anion is the best of these three imide ligands at stabilising the lower M^{II} oxidation state. This is also consistent with the expectation that of these three imide ligands the pyrazine-pyrazine dpzca anion is the poorest σ-donor and best π-acceptor, whereas the pyridine-pyridine bpca anion is the best σ-donor and poorest π-acceptor. Replacing the first two coordinated pyridine rings with pyrazine rings increases E$_m$(M$^{II/III}$) by about +0.1 to +0.2 V, and the second two by another +0.15 to +0.24 V, which may be useful for the informed design and tuning of electrochemical properties in future systems.

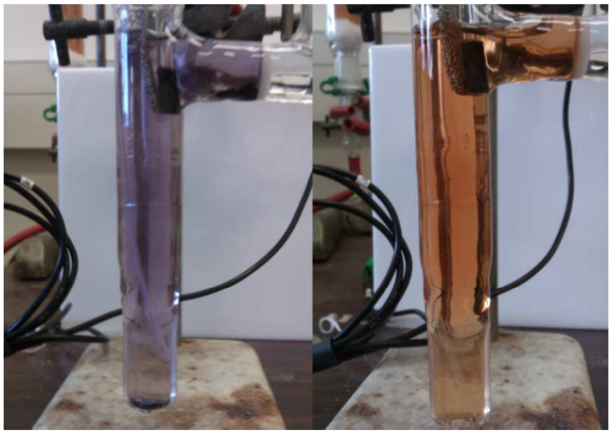

Fig. 7. The reversible colour change observed during the oxidation of [Fe^{II}(dpzca)$_2$] (left) to [Fe^{III}(dpzca)$_2$]$^+$ (right). Controlled potential electrolysis was performed at 0.65 V vs 0.01 M AgNO$_3$/Ag, on 10 mL of a 0.518 mmol L^{-1} suspension of [Fe^{II}(dpzca)$_2$] in acetonitrile, resulting in the transfer of 0.94 electron equivalents per mole.

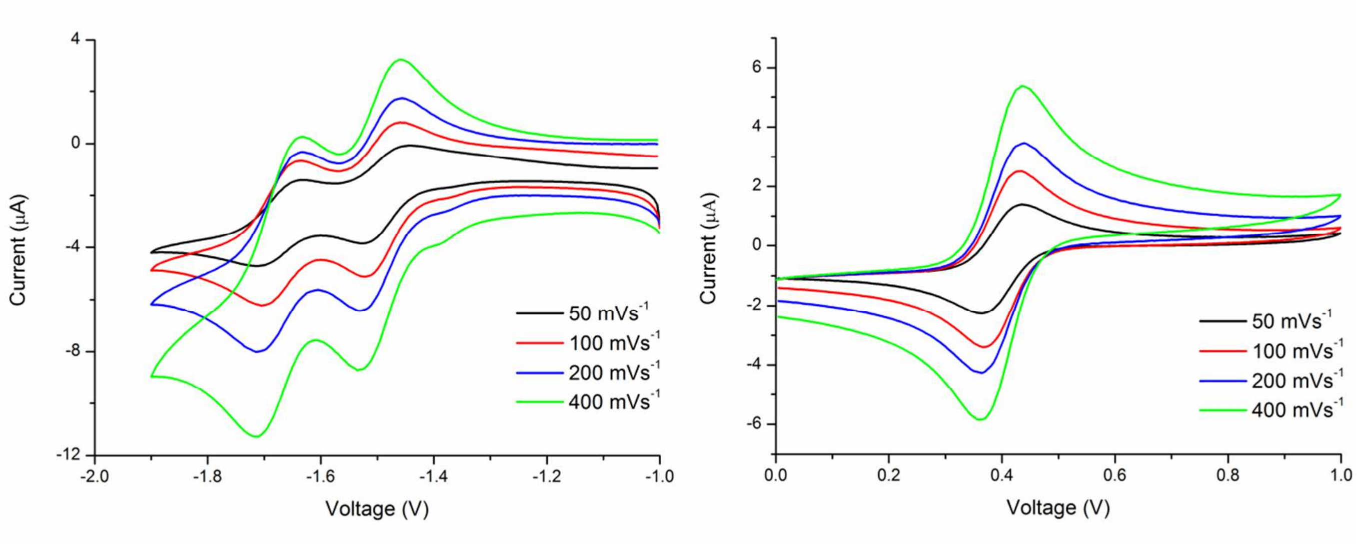

Fig. 8 A scan rate study on a 0.518 mmol L^{-1} solution of [Fe^{III}(dpzca)$_2$]$^+$ in acetonitrile (after bulk electrolysis of a suspension of [Fe^{II}(dpzca)$_2$] at 0.65 V passed 0.94 electron equivalents per mole) of (left) the ligand-based processes (-1→-1.9→-1 V) and (right) the reversible metal based processes (0→1.0→0 V). Reference 0.01 M AgNO$_3$/Ag.

Table 2 E$_m$ (V) and [ΔE] (mV) values in acetonitrile for the [M(dpzca)$_2$] complexes reported in this work (referenced to 0.01 M Ag$^+$/AgNO$_3$).

M$^{II/III}$	E$_m$ [ΔE] for [M(dpzca)$_2$]		
	Metal Based Process	**1st Ligand Reduction**	**2nd Ligand Reduction**
Fe[a]	0.40 [70]	-1.49 [70]	-1.67 [80]
Co[b, ref 12]	-0.22 [61]	-1.46 [71]	-1.84 [77]
Ni[c]	0.96 [43]	-1.60 [22]	-1.78 [63]
Cu	-0.79[d]		
Zn		-1.62 [30]	-1.77 [18]

[a] After bulk electrolysis at 0.65 V transferred 0.94 electron equivalents. [b] After bulk electrolysis at 0.0 V transferred 1.04 electron equivalents. [c] After bulk electrolysis to 1.1 V transferred 0.95 electron equivalents. [d] This process is very weak, due to the low solubility of this complex (see ESI).

Table 3 The differences in E$_m$ (V) for the metal based processes of the mononuclear complexes [M(bpca)$_2$],[29] [M(pypzca)$_2$],[11] and [M(dpzca)$_2$].

M$^{II/III}$	E$_m$ for [M(bpca)$_2$][29]	Δ	E$_m$ [ΔE] for [M(pypzca)$_2$][11]	Δ	E$_m$ [ΔE] for [M(dpzca)$_2$] (present work)
Cr	(-0.74) -1.072[a]				
Fe	(+0.35) +0.048[a]	0.11	+0.16 [73]	0.24	0.40 [70]
Co	(-0.28) -0.582[a]	0.21	-0.37 [79]	0.15	-0.22 [61]
Ni			+0.78 [68]	0.18	0.96 [43]

[a] The values in brackets were recorded as 1 mM solutions in a 0.1 M nBu$_4$NPF$_6$ acetonitrile solution using a glassy carbon electrode at a scan rate of 50 mVs^{-1} vs. SSCE. In order to compare these SSCE referenced literature values with those recorded for the [M(pypzca)$_2$] and [M(dpzca)$_2$] complexes which used a 0.01 M Ag$^+$/AgNO$_3$ reference, 0.302 V has been subtracted from the literature values.[30]

Table 4 The differences in E$_m$ (V) for the first ligand-based processes of the mononuclear complexes [M(bpca)$_2$],[29] [M(pypzca)$_2$],[11] and [M(dpzca)$_2$].

M$^{II/III}$	E$_m$ for [M(bpca)$_2$][29]	Δ	E$_m$ [ΔE] for [M(pypzca)$_2$][11]	Δ	E$_m$ [ΔE] for [M(dpzca)$_2$]
Cr	(-1.47) -1.77[a]				
Fe			-1.64 [70]	0.15	-1.49 [70]
Co	(-1.66) -1.96[a]	0.4	-1.56 [70]	0.1	-1.46 [71] [ref 12]
Ni			-1.72 [78]	0.12	-1.60 [22]
Zn			-1.72 [81]	0.1	-1.62 [30]

[a] The values in brackets were recorded as 1 mM solutions in a 0.1 M nBu$_4$NPF$_6$ acetonitrile solution using a glassy carbon electrode at a scan rate of 50 mVs^{-1} vs. SSCE. In order to compare these SSCE referenced literature values with those recorded for the [M(pypzca)$_2$] and [M(dpzca)$_2$] complexes which used a 0.01 M Ag$^+$/AgNO$_3$ reference, 0.302 V has been subtracted from the literature values.[30]

Magnetic Properties

To our knowledge, $[\mathrm{Co^{II}(dpzca)_2}]$ is only the second cobalt(II) imide complex which has been reported in the literature,[1] the first being the analogous complex, $[\mathrm{Co^{II}(pypzca)_2}]$, of the non-symmetric pyridine/pyrazine imide ligand.[11] As we reported earlier, whilst the latter is high spin throughout the temperature range studied,[11] the former exhibits remarkable magnetic properties (pressure and temperature induced spin crossover with hysteresis; and reversible redox properties).[12, 13]

Both $[\mathrm{Fe^{II}(dpzca)_2}]$ and $[\mathrm{Co^{III}(dpzca)_2}]\mathrm{BF_4}$ are low spin and hence diamagnetic at room temperature. The room temperature μ_{eff} values for $[\mathrm{Ni^{II}(dpzca)_2}]$ (3.3 BM) and $[\mathrm{Cu^{II}(dpzca)_2}]$ (2.2 BM) are within the range expected for two and one unpaired electron, respectively.

Supramolecular architectures: secondary assembly of SBUs

The $[\mathrm{M^{II/III}(dpzca)_2}]\mathrm{X_n}$ building block complexes with M = $\mathrm{Co^{II/III}}$ or $\mathrm{Ni^{II}}$ were successfully assembled with silver(I) tetrafluoroborate to form $\mathrm{CO_2}$-selective MOFs.[10] Hence assembly of these two SBUs using a different silver(I) salt, specifically silver(I) nitrate, were carried out in order to test whether or not analogous MOFs with nitrate instead of tetrafluoroborate anions in the channels, could be accessed. However, unlike the previously reported assembly reactions with silver tetrafluoroborate, the reactions with silver nitrate did not produce a pair of isostructural $\mathrm{Co^{III}}$ and $\mathrm{Ni^{II}}$ MOFs. Rather, the reaction of $[\mathrm{Co^{II}(dpzca)_2}]$ resulted in the 3D framework $\{[\mathrm{Co^{III}(dpzca)_2Ag^{I}}](\mathrm{NO_3})_2\}_n\cdot 2\mathrm{H_2O}$ (**3**), that is structurally distinct from those previously reported (Fig. 9-10). In contrast, the reaction of $[\mathrm{Ni^{II}(dpzca)_2}]$ with silver nitrate in 1:1 water/acetone resulted in some green single crystals of a 1D chain, $\{([\mathrm{Ni^{II}(dpzca)_2Ag^{I}_{½}}](½\mathrm{NO_3})(x\mathrm{H_2O}\}_n$ (**4**) (Fig. 11 and S1).

The new nitrate-containing MOF, **3**, crystallised in the monoclinic space group *P*2$_1$/*m* rather than the orthorhombic *Cmcm* observed for the pair of previously reported tetrafluoroborate-containing MOFs, $\{[\mathrm{Co^{III}(dpzca)_2Ag}](\mathrm{BF_4})_2\cdot(\mathrm{H_2O})_2\}_n$ (**1**) and $\{[\mathrm{Ni^{II}(dpzca)_2Ag}](\mathrm{BF_4})\ (\mathrm{acetone})_{0.5}\}_n$ (**2**), but overall is otherwise quite similar (Fig. 9, top). As was observed for **1** and **2**, the silver(I) linker in **3** adopts a rare $\mathrm{N_4O_2}$ donor set through coordination to the 'spare' pyrazine nitrogen atoms on four of the adjacent SBUs and to a pair of 'spare' bidentate imide oxygen atoms on a fifth adjacent SBU (Fig. 12). The remaining 'spare' imide oxygen pair on each SBU forms one wall of the anion containing channels through non-classical C-H···O hydrogen bonds with the hydrogen atoms on adjacent pyrazine rings [C(H)···O 3.009(11) Å, 179.6°; C(H)···O 3.271(11) Å, 154.2°].

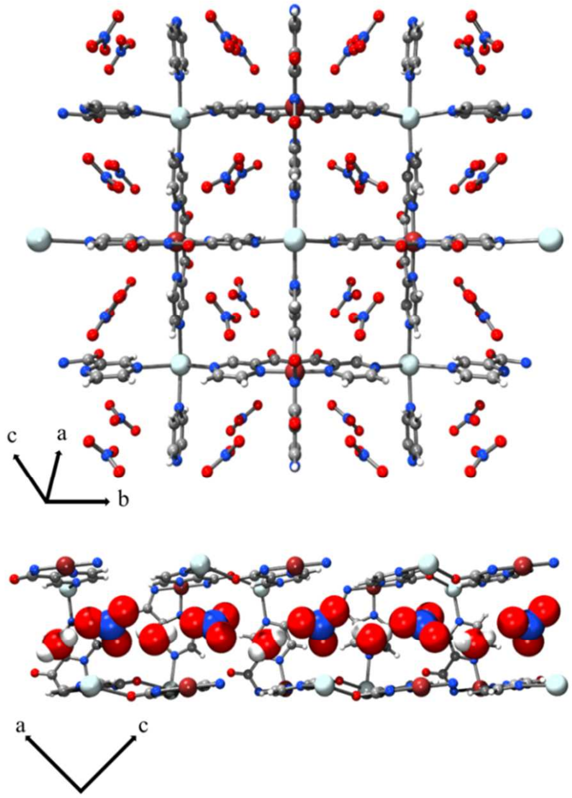

Fig. 9. Perspective views of the 3D framework $\{[\mathrm{Co^{III}(dpzca)_2Ag^{I}}](\mathrm{NO_3})_2\}_n\cdot 2\mathrm{H_2O}$ (**3**), showing only one component of the solvent and anion disorder (in the channels) for clarity. Top: looking down the channels at an angle of 45° to the crystallographic a-axis. Bottom: a channel running left to right, viewed down the b-axis.

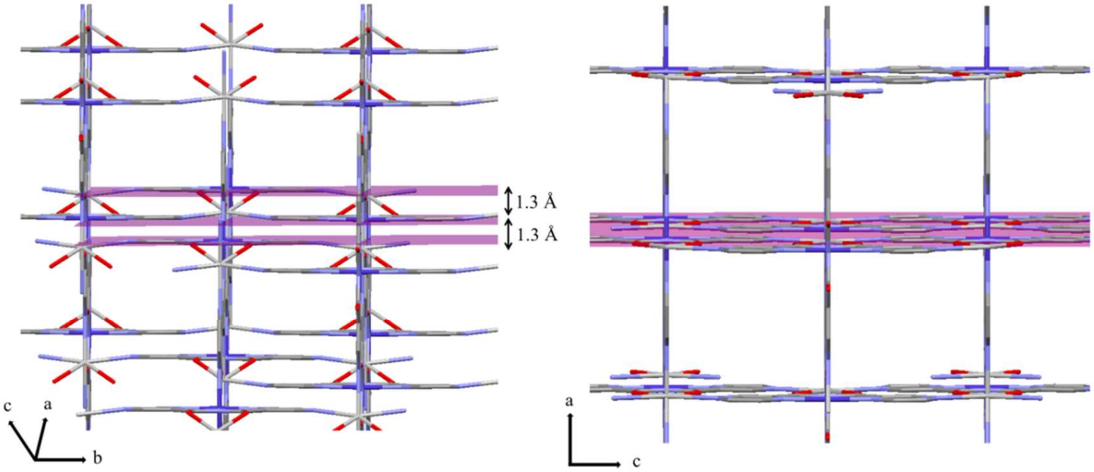

Fig. 10. Views showing (left): the stepping of the SBUs by 1.3 Å down the channels in nitrate MOF **3** (viewed with the plane of the page bisecting the a- and c-axes in the vertical, and the b-axis horizontal), as compared to (right) the corresponding view of tetrafluoroborate MOF **1** (as viewed down the b-axis). The mean planes indicated in magenta are defined by the pyrazine rings in each case. The anions are omitted for clarity.

Table 5. Selected structural comparisons (distances in Å; angles in °) between the two new architectures and those previously reported.[10]

	$\{[Co^{III}(dpzca)_2Ag](BF_4)_2\cdot(H_2O)_2\}_n$ (**1**)	$\{[Ni^{II}(dpzca)_2Ag](BF_4)\cdot(acetone)_{0.5}\}_n$ (**2**)	$\{[Co^{III}(dpzca)_2Ag^I](NO_3)_2\cdot2(H_2O)\}_n$ (**3**)	$\{([Ni^{II}(dpzca)_2Ag^I_{½}](½NO_3)(xH_2O\}_n$ (**4**)
Type	3D Framework	3D Framework	3D Framework	1D Chain
Crystal system	Orthorhombic	Orthorhombic	Monoclinic	Monoclinic
Space Group	*Cmcm*	*Cmcm*	$P2_1/m$	$C2/m$
a,b,c (Å)	13.708(3), 14.079(2), 13.798(3)	14.0140(14), 14.4385(14), 13.6760(14)	9.3678(4), 13.6094(6), 10.1421(4)	14.619(3), 24.806(4), 9.861(4)
β (°)	90	90	90.273(2)	122.003(7)
V ($Å^3$)	2663.1(10)	2767.2(5)	1293.00(9)	3032.2(14)
Ag coordination	N_4O_2 octahedral	N_4O_2 octahedral	N_4O_2 octahedral	N_4 square planar
Average Ag–N length	2.472	2.483	2.441	2.367
Average Ag-O length	2.449	2.552	2.568	N/A
Ag distortion parameter[a]	$\sum = 97.94$	$\sum = 72.05$	$\sum = 131.8$	$\tau_4 = 0$

[a] Either the octahedral distortion parameter, ∑ (the sum of the absolute values of the difference of each of the 12 cis angles from 90°; 0 for a perfect octahedron), or the square planar/tetrahedral distortion parameter, τ_4 (1 for tetrahedral, 0 for square planar),[33] as appropriate.

The key difference seen for the nitrate-containing MOF **3** is that the Ag(I) linker has a significantly greater octahedral distortion parameter than it does in the previously reported tetrafluoroborate MOFs **1** and **2** (Fig. 12, Table 5). This is due to sequential ligand planes of the SBU perpendicular to the *a,c* diagonal stepping by 1.3 Å per plane/cobalt centre along that diagonal. This is seen most clearly when viewed either down the resulting sloping channels (Fig. 10) or viewed side-on noting the angled channel roof and floor components (Fig. 9, bottom), and comparing these with those in MOF **1**. There is no guest accessible void volume in the as-synthesised structure. The asymmetric unit of MOF **3** contains one nitrate anion disordered over two half occupancy sites and a single water molecule is disordered over the same two sites. The closest O···O distances—between adjacent partial occupancy nitrate sites is very short [1.89(2) and 2.03(2) Å] so no two adjacent sites would be occupied at the same time within a single channel. Rather, the half occupancy nitrate anions alternate with the half occupancy water molecules as shown (Fig. 9 bottom), with the other component of the disorder similar, but with their relative positions reversed. This facilitates H-bonds between them [$O_{31}\cdots(H)O_{61}$ 3.16(2) Å, 123°; $O_{41}\cdots(H)O_{61}$ 2.77(2) Å, 134°; $O_{33}\cdots(H)O_{51}$ 2.89(2) Å, 170°; $O_{42}\cdots(H)O_{51}$ 3.05(2) Å, 178°].

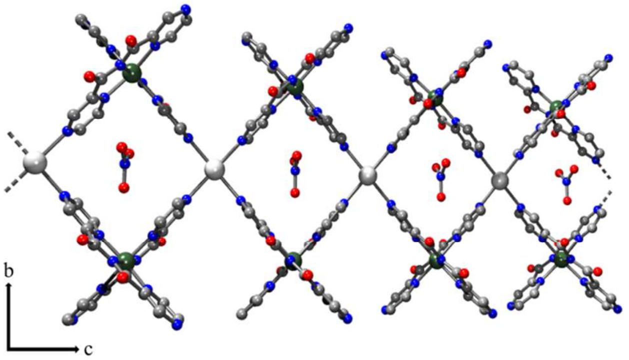

Fig. 11. Perspective view of the 1D chain $\{([Ni^{II}(dpzca)_2Ag^I_{½}](½NO_3)(xH_2O\}_n$ (**4**) in the *bc* plane. Showing only one component of the four-fold anion disorder; waters of crystallisation absent as Platon SQUEEZE was applied.[31, 32]

The asymmetric unit of the 1D chain, **4**, comprises a half occupancy nickel centre (2 fold axis), one full imide ligand, a quarter occupancy silver centre (2/m site) and a quarter occupancy nitrate ion (N31 atom on a mirror plane; O32 on a two-fold axis at right angles to the mirror plane; symmetry therefore generates four quarter occupancy nitrates in the same region of space, only one of which can be present at any one time). Applying the symmetry elements generates a 1D chain (Fig. 11) with almost-square pockets [N_{pz1} – Ni1 – N_{pz1A} 89.58°; N_{pz2} – Ag1 – N_{pz2}, 94.74°; Ni1···Ag1 = Ni1A···Ag1 7.203(10) Å], generated from linking a pair of nickel(II) building block complexes via a silver(I) linker to the next pair, that accommodate the disordered nitrate anions. The disordered water molecules of solvation could not be resolved so SQUEEZE was applied, resulting in an electron count (50) consistent with the presence of approximately 4-5 water molecules per Ni^{II} ion.

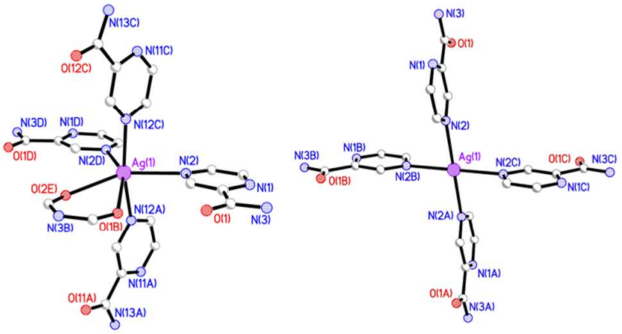

Fig. 12. Perspective views highlighting the differing coordination spheres of the silver(I) connectors, which are comprised of some of the 'spare' donors of the $[M^{II/III}(dpzca)_2]^{0/+}$ building blocks, present in the coordination polymers: 3D MOF **3** (M = Co^{III}, left, N_4O_2) and 1D linear chain polymer **4** (M = Ni^{II}, right, N_4).

In contrast to MOFs **1**-**3**, the silver(I) linker in the 1D chain polymer **4** binds *only* to the 'spare' pyrazine nitrogen atom (N2) (Fig. 12) on each of four symmetry generated adjacent building block complexes (2 on each side), giving an N_4-donor *square planar* coordination. The result is a straight, square 'concertina' type structure with the silver and nickel ions as the 'hinges', and each silver ion bridging four building block complexes. Within the SBUs, the nickel(II) centres coordinate to four pyrazine nitrogens (N1, N1A, N5, N5A) and two imide nitrogen atoms (N3, N3A), retaining an octahedral N_6-donor coordination environment.

Also in contrast to **1**-**3** in which the M:Ag molar ratio is 1:1, this ratio is 2:1 in **4**, which leaves two 'spare' nitrogen atoms per SBU (N4, N4A) that remain uncoordinated. These are instead involved in weak, non-classical H-bonds with C1 and C2 of a pyrazine ring on the adjacent chain [$C_1(H)\cdots N_4$ 3.127(7) Å, 113.4°; $C_2(H)\cdots N_4$ 3.391(9) Å, 98.4°]. The 'spare' imide oxygen atoms also remain uncoordinated, and instead form bifurcated, non-classical, O···H-C hydrogen bonds with pyrazine hydrogens on adjacent 1-D chains [$C_{10}(H)\cdots O_1$ 3.249(7) Å, 151.4°; $C_{10}(H)\cdots O_2$ 3.089(10) Å, 134.4°] (Fig. S2).

Conclusion

The synthesis and structures of four new building block complexes of the symmetric pyrazine-based imide ligand Hdpzca are detailed herein. Structural analysis of these complexes has shown that the secondary assembly instructions, in the form of four 'spare' pyrazine nitrogen atoms and two pairs of 'spare' imide oxygen atoms, are positioned in an approximately octahedral arrangement. This facilitates the use of these complexes as building blocks for the production of larger discrete or polymeric assemblies, as demonstrated herein by the reaction of $[Co^{II}(dpzca)_2]$ and $[Ni^{II}(dpzca)_2]$ with silver nitrate to give the 3D MOF $\{[Co^{III}(dpzca)_2Ag^{I}](NO_3)_2\cdot 2(H_2O)\}_n$ (**3**) and the 1D chain coordination polymer $\{([Ni^{II}(dpzca)_2Ag^{I}_{½}](½NO_3)(xH_2O\}_n$ (**4**), respectively. In both cases each $[M^{II}(pypzca)_2]^{+/0}$ SBU has N_4O_4 secondary donors available: the different structural types come about due to the silver(I) connector using all but two imide oxygen atoms in forming **3**, giving it an N_4O_2 environment, but using only two of the pyrazine nitrogen donors, giving it an N_4 environment, in forming **4**. The difference in donor type between the oxygen and nitrogen secondary donor sets also offers the future possibility of an elegant, stepwise assembly of larger structures by judicious choice of linking metal ions.

As for the previously reported pyridine-pyrazine imide complexes $[M^{II}(pypzca)_2]$,[11] the very low solubility of the all-pyrazine analogues, $[M^{II}(dpzca)_2]$, was overcome by using bulk electrolysis to first prepare the soluble $[M^{III}(dpzca)_2]^+$ complexes in situ. For the *all pyrazine* $[M^{II}(dpzca)_2]$ complexes the quasi-reversible metal based processes were observed at potentials between 0.15-0.24 V higher than those reported for complexes of Hpypzca (*pyridine/pyrazine*) and 0.35-0.36 V higher than those reported for complexes of Hbpca (*all pyridine*). This indicates that the electronic differences imposed on the metal centre by a coordinated pyrazine rather than a pyridine ring is equivalent to lifting the $E_m(M^{II/III})$ by about 0.1 V per ring, significantly increasing the stability of the +2 oxidation state over the +3. This information may be useful for the fine tuning of electron density dependent properties of such complexes for future applications as catalysts or spin crossover-based nanocomponents.

Experimental

General procedures

Unless otherwise stated, all reagents (including 2-pyrazine carboxylic acid and 2-pyrazine carboxamide) and solvents were commercially available and used as received. If desired, 2-pyrazine carboxamide can be prepared from 2-pyrazine carboxylic acid as described below. Dry toluene was obtained from a MD-6 solvent purification system. Acetonitrile and triethylamine were both distilled over calcium hydride before use. Powder samples of $[Ni^{II}(dpzca)_2]$ and $[Co^{III}(dpzca)_2](BF_4)$ were prepared as described elsewhere.[10]

Instrumentation and measurements

Infrared spectra were recorded on a Bruker Alpha-P diamond anvil system. NMR spectra were recorded on a Varian 500 MHz Ar spectrometer. Mass spectra were recorded on a Bruker MicrOTOF-Q spectrometer. Microanalysis was performed by the Campbell Microanalytical Laboratory at the University of Otago. UV-Vis spectra were recorded on a JASCO V550 Spectrophotometer. Room temperature magnetic moments were recorded on an Alfa Products MK I Magnetic Susceptibility Balance or a Quantum Design Physical Property Measurement System equipped with a vibrating sample mount, using an applied field of 0.1 Tesla at Industrial Research Limited (IRL; now RRI Robinson Research Institute) Lower-Hutt, New Zealand.

X-ray data were collected on a Bruker APEX II area detector diffractometer at the University of Otago using graphite-monochromated $Mo_{K\alpha}$ radiation (λ = 0.71073 Å). The data were corrected for Lorentz and polarisation effects, and semi-empirical absorption corrections (SCALE) were applied. The structures were solved by direct methods (SHELXS-97)[34] and refined against all F^2 data (SHELXL-97).[35, 36] Other than the exceptions noted in the CIF files, the hydrogen atoms were inserted at calculated positions and rode on the atoms to which they were attached and all non-hydrogen atoms were made anisotropic. Crystal structure determination details are summarized in Tables S6-S7. The Cambridge CCDC 1030793-1030799 contains the supplementary crystallographic data for this paper and can be obtained free of charge via www.ccdc.cam.ac.uk/data_request/cif.

Electrochemistry samples were 10 mL of a 1 mmol L^{-1} solution or suspension (see Figure captions) in dried acetonitrile (freshly distilled from CaH_2) with 0.1 mol L^{-1} tetrabutylammonium hexafluorophosphate as the supporting electrolyte. Data were collected under an argon atmosphere on an EG & G Princeton Applied Research Potentiostat/Galvanostat Model 273A, using PowerSuite V2.58 software. The working electrode was a 1 mm diameter Pt disk electrode and the reference electrode was Ag/Ag^+ (0.01 mol L^{-1} $AgNO_3$ in 0.1 mol L^{-1} tetrabutylammonium hexafluorophosphate with acetonitrile as the solvent). The Fc/Fc^+ couple was consistently observed at E_m = 0.100±0.005 V with a ΔE_P of 0.081 V. E_m is the midpoint potential (approximately the reversible formal potential), calculated from the average of E_{PA} and E_{PC}. ΔE_P is the absolute value of the difference between E_{PA} and E_{PC}.

2-Pyrazinecarboxamide·H_2O

2-Pyrazine carboxylic acid (100 mg, 0.806 mmol) was suspended in ammonium hydroxide (5 mL) and stirred at room temperature for 12 hours. To the resulting clear colourless solution was added acetone (25 mL) causing immediate precipitation of 2-pyrazinecarboxamide as a white microcrystalline solid which was filtered and washed with acetone (3 x 25 mL), air dried and then further dried *in vacuo* (94.3 mg ,0.766 mmol, 95%) Elemental analysis calcd (%) for $C_6H_7N_2O_3$ (139.113 g mol^{-1}): Calc. C 42.55, H 5.00, N 29.77; found: C 42.58, H 5.06, N 29.77. ^{1}H NMR (400 MHz, CDCl$_3$): δ (ppm) 9.42 (d, $J_{3\text{-}2}$ = 1.5 Hz 1H, H_3), 8.78 (d, $J_{1\text{-}2}$ = 2.5 Hz, 1H, H_1), 8.56 (dd, $J_{2\text{-}1}$ = 2.5 Hz, $J_{2\text{-}3}$ = 2.5 Hz 1H, H_2), 7.63 (br s, 1H, H_{4a}), 5.70 (br s, 1H, H_{4b}).

N-(2-Pyrazylcarbonyl)-2-pyrazinecarboxamide (Hdpzca)

Method A. 2-Pyrazine carboxylic acid (0.978 g, 7.88 mmol) was dissolved in thionyl chloride (10 mL) and refluxed at 120 °C for two hours. The dark purple solution was then evaporated under reduced pressure and the resulting solid was dissolved in dry toluene (20 mL). 2-Pyrazine carboxamide (0.530 g, 4.27 mmol) was then added and the resulting suspension was refluxed at 120 °C for 3 days. The resulting solution was evaporated and the collected solids were redissolved in dichloromethane and filtered through celite to remove the purple contaminants. The filtrate was evaporated to dryness and the solids were purified by column chromatography with 1:1 dichloromethane/acetone on silica gel (R_f = 0.72). Hdpzca was collected as an off white solid (0.663 g, 67%). MS (+ESI) (Acetone): m/z 252.0483 [$C_{11}H_8N_4O_2Na$]$^+$ calc. 252.0492. Elemental analysis calcd (%) for $C_{10}H_6N_5O_2$ (229.06): Calc. C 52.40 H 3.08 N 30.56; found: C 52.22 H 3.06 N 30.31. IR: ν / cm^{-1} = 3290, 1757, 1579, 1527, 1462, 1411, 1396, 1288, 1240, 1173, 1127, 1069, 1017, 869, 819, 762, 719, 650, 614, 437. ^{1}H NMR (500 MHz, d$_6$-DMSO): δ (ppm) 12.42 (s, 1H, H_4), 9.38 (d, $J_{3\text{-}2}$ = 1.2 Hz, 1H, H_3), 9.05 (d, $J_{1\text{-}2}$ = 2.4 Hz, 1H, H_1), 8.91 (dd, $J_{2\text{-}1}$ = 2.4 Hz, $J_{2\text{-}3}$ = 1.5 Hz, 1H, H_2). ^{13}C NMR (500 MHz, d$_6$-DMSO): δ (ppm) 160.9 (C_E), 149.2 (C_A), 144.4 (C_C), 143.6 (C_B), 142.9 (C_D).

Method B. Pyrazine carboxylic acid (1.606 g, 13.1 mmol) was dissolved in thionyl chloride (10 mL) and refluxed at 120 °C for two hours. The dark purple solution was then evaporated under reduced pressure and the resulting solid dissolved in dry toluene (20 mL). 2-Pyrazinecarboxamide (1.13 g, 9.11 mmol) was then added and the resulting suspension was refluxed at 120 °C for 3 days. In a separate flask, pyrazine carboxylic acid (0.960 g, 7.8 mmol) was dissolved in thionyl chloride (5 mL) and refluxed at 120°C for two hours, evaporated to dryness under reduced pressure and the resulting purple solids were added to the first reaction solution. Refluxing at 120°C was continued for three more days. Methanol (20 mL) was added to the reaction solution and it was stirred for two hours. The solution was evaporated to dryness then dissolved in dichloromethane and filtered through celite to remove the purple contaminants. The filtrate was evaporated to dryness again, and then acetone (100 mL) was added. The resulting suspension was shaken, sonicated, then filtered to produce Hdpzca (1.632 g, 77%). Elemental analysis calcd (%) for $C_{10}H_6N_5O_2\cdot 0.2H_2O$ (232.66): Calc. C 51.59 H 3.20 N 30.08; found: C 51.59 H 3.20 N 30.08. ^{1}H NMR (300 MHz, d$_6$-DMSO): δ (ppm) 9.39 (d, $J_{3\text{-}2}$ = 0.9 Hz, 1H, H_3), 9.06 (d, $J_{1\text{-}2}$ = 1.8 Hz, 1H, H_1), 8.91 (dd, $J_{2\text{-}1}$ = 1.8 Hz, $J_{2\text{-}3}$ = 0.9 Hz, 1H, H_2).

(2-Pyrazylmethyl)-2-pyrazinecarboxamide (HL)

A solution of pyrazine-2-carboxylate (2.0 g, 14.5 mmol) and 2-aminomethylpyrazine (1.5 mL, 13.2 mmol) in methanol (80 mL) was refluxed for one week. The solution was evaporated to dryness and the solid purified by column chromatography using 5% methanol/dichloromethane on silica gel (R_f = 0.66). The product was collected as a white solid (2.37 g, 83%). MS (+ESI) (Methanol): m/z 238.0712 [$C_{10}H_9N_5ONa$]$^+$ calc. 238.0699. Elemental analysis calcd (%) for $C_{10}H_9N_5O$) (215.21 g mol^{-1}): Calc. C 55.81 H 4.22 N 35.24; found: C 55.92 H 4.23 N 32.76. IR: ν / cm^{-1} = 3087, 1719, 1654, 1605, 1585, 1411, 1325, 1028, 632. ^{1}H NMR (400 MHz, CDCl$_3$): δ (ppm) 9.43 (dd, $J_{3\text{-}2}$ = 1.2 Hz, $J_{3\text{-}1}$ = 0.4 Hz, 1H, H_3), 8.77 (dd, $J_{1\text{-}2}$ = 2.4 Hz, $J_{1\text{-}3}$ = 0.4 Hz, 1H, H_1), 8.68 (d, $J_{6\text{-}7}$ = 0.8 Hz, ½ 2H, H_6), 8.66 (s(br), ½ 2H, H_4), 8.56 (m, 2H, $H_{2/8}$), 8.52 (d, $J_{7\text{-}8}$ = 2.8 Hz, 1H, H_6), 4.85 (d, $J_{5\text{-}4}$ = 4.2 Hz, 2H, H_5). ^{13}C NMR (400 MHz, CDCl$_3$): δ (ppm) 169.9 (C_E), 152.2 (C_D), 147.5 (C_A), 144.5 (C_C), 144.2(C_G), 144.0 (C_B), 143.9 (C_H), 143.7 (C_J), 142.9 (C_I), 42.4 (C_F).

[Fe^{II}(dpzca)$_2$]

Solutions of Hdpzca (96.6 mg, 0.422 mmol) in dichloromethane (5 mL) and iron(II) tetrafluoroborate hexahydrate (74 mg, 0.219 mmol) in methanol (5 mL) were mixed thoroughly and put in one arm of an H-tube. Triethylamine (3-5 mL) was then placed in the other arm and the tube was sealed. The triethylamine vapour then diffused into the mixture and the resulting dark purple crystals were isolated by filtration and washed with water and dichloromethane, then dried under vacuum to yield [Fe^{II}(dpzca)$_2$] (106 mg, 94%). MS (+ESI) (CH$_2$Cl$_2$): m/z 535.0237 [Fe($C_{10}H_6N_5O_2$)$_2$Na]$^+$ calc. 535.0285, 513.0386 [Fe($C_{10}H_6N_5O_2$)$_2$H]$^+$ 513.0465. Elemental analysis calcd (%) for [Fe($C_{10}H_6N_5O_2$)$_2$] (512.22 g mol^{-1}): Calc. C 46.90 H 2.36 N 27.34; found: C 46.90 H 2.46 N 27.51. IR: ν / cm^{-1} = 3086 (w), 3053 (w), 1692 (s), 1609 (s), 1577 (m), 1518 (w), 1407 (s), 1312 (m), 1255 (s), 1198 (m), 1170 (m), 749 (s), 656 (s). (SQUID, 298 K) 0 BM (diamagnetic). UV-Vis (CH$_3$NO$_2$): ε_{514} = 9636, ε_{567} = 6568, ε_{690} = 1920 L cm^{-1} mol^{-1}.

{[Co^{III}(dpzca)$_2$](BF$_4$)}$_2$·5MeCN

Solid silver tetrafluoroborate (13.4 mg, 0.0688 mmol) was added to an orange solution of [Co^{II}(dpzca)$_2$] (17.4 mg, 0.0289 mmol) in acetonitrile. No immediate colour change was observed and the solution was stirred at ambient temperature for 12 hours before being subjected to vapour diffusion of diethyl ether. After 2 weeks a few orange plate shaped crystals suitable for X-ray crystallography were obtained. Due to the low yield (<1 mg) and obvious physical contaminants these were only characterised by X-ray crystallography.

[Cu^{II}(dpzca)$_2$]

A solution copper(II) tetrafluoroborate hexahydrate (81.7 mg, 0.244 mmol) in acetone (10 mL) was added to a suspension of Hdpzca (110.4 mg, 0.482 mmol) (10 mL) and dichloromethane (2 mL) with triethylamine (67 µL, 0.481 mmol). After two hours the resulting green solid was filtered dried under vacuum to yield [Cu^{II}(dpzca)$_2$] (106.8 mg, 84%). MS (+ESI) (CHCl$_3$/CH$_3$OH): m/z 542.0264 [Cu($C_{10}H_6N_5O_2$)$_2$Na]$^+$ calc. 542.0231, 290.9829 [Cu($C_{10}H_6N_5O_2$)]$^+$ 290.9812, 252.0507 [($C_{10}H_7N_5O_2$)Na]$^+$

252.0492. Elemental analysis calcd (%) for [$Cu^{II}(C_{10}H_6N_5O_2)_2$] (515.07 g mol^{-1}): Calc. C 46.20 H 2.35 N 27.18; found: C 46.09 H 2.27 N 26.94. IR: ν / cm^{-1} = 3096 (w), 3061 (w), 3024 (w), 1701 (s), 1696 (m), 1617 (m), 1581 (w), 1528 (m), 1320 (s), 1278 (m), 1151 (s), 1030 (s), 818 (m), 649 (m). μ_{eff} (Johnson-Matthey, 298 K) = 2.2 BM. UV-Vis (CH_3NO_2): ε_{626} = 317 L cm^{-1} mol^{-1}.

[Zn^{II}(dpzca)$_2$]

A solution of zinc(II) tetrafluoroborate hydrate (58.3 mg, 0.244 mmol) in methanol (10 mL) was added to a solution of Hdpzca (105.4 mg, 0.460 mmol) in dichloromethane (20 mL) with triethylamine (64 μL, 0.460 mmol). After two hours the resulting white solid was filtered and dried under vacuum to yield [Zn^{II}(dpzca)$_2$] (56.1 mg, 44%). MS (+ESI) (CH_3OH): m/z 543.0131 [$Zn(C_{10}H_6N_5O_2)_2Na$]$^+$ calc. 543.0227, 252.0455 [($C_{10}H_7N_5O_2$)Na]$^+$ 252.0492. Elemental analysis calcd (%) for [$Zn^{II}(C_{10}H_6N_5O_2)_2$] (521.76 g mol^{-1}): Calc. C 46.04 H 2.32 N 26.85; found: C 46.12 H 2.15 N 26.70. IR: ν / cm^{-1} = 1699 (s), 1617 (m), 1582 (w), 1528 (w), 1468 (m), 1402 (m), 1324 (s), 1279 (m), 1201 (m), 1152 (m), 1085 (w), 1038 (s), 983 (w), 789 (m), 649 (m), 631 (s), 454 (s).

[Cu^{II}(dpzca)(H_2O)$_2$]$BF_4\cdot H_2O$

Hdpzca (13.9 mg, 0.061 mmol) was dissolved in dichloromethane (5 mL) and mixed with a solution of copper(II) tetrafluoroborate hydrate (58.0 mg, 0.253 mmol) in methanol (5 mL). The resulting suspension of blue-green solid was filtered after five hours, subsequent recrystallisation by slow evaporation from water yielded [Cu^{II}(dpzca)(H_2O)$_2$]$BF_4\cdot H_2O$ (24.1 mg, 91%). MS (+ESI) (CH_3OH): m/z 313.9724 [$Cu(C_{10}H_6N_5O_2)Na$]$^+$ 303.9710, 290.9803 [$Cu(C_{10}H_6N_5O_2)$]$^+$ 290.9812, 229.9605 [($C_{10}H_7N_5O_2$)H]$^+$ 230.0673. Elemental analysis calcd (%) for [$Cu^{II}(C_{10}H_6N_5O_2)(H_2O)_2$]$BF_4\cdot H_2O$ (432.58 g mol^{-1}): Calc. C 29.62 H 2.24 N 17.27; found: C 29.98 H 2.07 N 16.86. IR: ν / cm^{-1} 3399 (w), 3230 (w), 3112 (w), 1715 (m), 1568 (m), 1473 (m), 1450 (m), 1076 (s), 1049 (s), 1003 (s), 762 (m), 638 (m). UV-Vis (H_2O): ε_{654} = 133; ε_{278} = 15,472; ε_{208} = 16,554 dm^{3}cm^{-1}mol^{-1}.

[Cu^{II}(dpzca)(H_2O)$_3$]$_2SiF_6$

Hdpzca (111.7 mg, 0.488 mmol) was dissolved in dichloromethane (10 mL) and mixed with a solution of copper(II) tetrafluoroborate hydrate (163.8 mg, 0.490 mmol) in methanol (10 mL). The resulting suspension of blue-green solid was stirred for five hours then evaporated to dryness. The solids were recrystallised from boiling water to yield dark green block shaped crystals a few of which were kept in the mother liquor for X-ray crystallography ([Cu^{II}_2(dpzca)$_2$(H_2O)$_3$]$SiF_6\cdot 2H_2O$). The rest were filtered, washed with cold H_2O and dried under vacuum for 5 days to yield [Cu^{II}_2(dpzca)$_2$(H_2O)$_3$]SiF_6 (62.4 mg, 29%). MS (+ESI) (CH_3OH): m/z 626.9616 [$Cu_2(C_{10}H_6N_5O_2)_2SiF$]$^+$ 626.9226, 308.9872 [$Cu(C_{10}H_6N_5O_2)$]$^+$ 308.9918, 290.9842 [($C_{10}H_7N_5O_2$)H]$^+$ 290.9812. Elemental analysis calcd (%) for [$Cu^{II}(C_{10}H_6N_5O_2)(H_2O)_3$]$_2SiF_6$ (833.6394 g mol^{-1}): Calc. C 28.82 H 2.90 N 16.80; found: C 29.12 H 3.06 N 16.69. IR: ν / cm^{-1} = 3351 (m), 3103 (w), 1719 (w), 1697 (m), 1654 (m), 1648 (m), 1344 (m), 1164 (m), 1082 (m), 1055 (m), 789 (m), 669 (s).

{[Co^{III}(dpzca)$_2Ag^I$](NO_3)$_2\cdot 2(H_2O)$}$_n$

The complex [Co^{II}(dpzca)$_2$] (71.2 mg, 0.138 mmol) was dissolved in 1:1 water/acetone (100 mL) and heated to 100 °C. A solution of silver(I) nitrate (193 mg, 1.14 mmol) in water (100 mL) was then added, resulting in an immediate precipitate. After approximately 30 minutes the suspension cleared and the solution was refluxed for a further 6 hours. The solution was then filtered through cotton wool into a conical flask wrapped in tinfoil and allowed to slowly evaporate. After 2 weeks red single crystals of {[Co^{III}(dpzca)$_2Ag^I$](NO_3)$_2\cdot 2(H_2O)$}$_n$ (**3**) suitable for X-ray crystallography were obtained. These were subsequently collected and air dried (87 mg, 78%). Elemental analysis calcd (%) for [$Co^{III}(C_{10}H_6N_5O_2)_2Ag^I$]($NO_3$)$_2$($H_2O$)$_3$($C_3H_6O$)$_{0.15}$ (809.95 g mol^{-1}): Calc. C 30.33 H 2.35 N 20.75; found: C 30.54 H 1.99 N 20.43. IR: ν / cm^{-1} = 3193 (m), 3089 (w), 1712 (m), 1697 (m), 1624 (m), 1289 (s, br), 1162 (m), 1083 (m), 1038 (m), 781 (m), 640 (m).

{([Ni^{II}(dpzca)$_2Ag^I_{½}$](½NO_3)(xH_2O}$_n$

The complex [Ni^{II}(dpzca)$_2$] (67.8 mg, 0.132 mmol) was dissolved in 100 mL of 1:1 acetone/water and heated to 120 °C. A solution of silver(I) nitrate (176 mg, 1.04 mmol) in water (50 mL) was then added and the resulting solution refluxed at 120 °C for 6 hours. The solution was then transferred to a conical flask wrapped in tinfoil and allowed to slowly evaporate. After 3 weeks some green single crystals of {([Ni^{II}(dpzca)$_2Ag^I_{½}$](½NO_3)(xH_2O}$_n$ (**4**) suitable for X-ray crystallography were obtained.

Acknowledgements

We thank the University of Otago for funding this research, including postgraduate scholarships to MGC and RGM. We are grateful to Scott A. Cameron for assisting with 'de-twinning' the structure of Hdpzca, Assoc. Prof. David S. Larsen for helpful discussions, and Dr Juan Olguín and Dr Humphrey L. C. Feltham for collecting the magnetic data. We thank the MacDiarmid Institute for funding the magnetometers and Dr Jeffrey L. Tallon for facilitating access to them, as well as the Campbell Microanalytical Laboratory (University of Otago) for performing the microanalyses.

Notes and references

[a] *Department of Chemistry and the MacDiarmid Institute for Advanced Materials and Nanotechnology, University of Otago, PO Box 56, Dunedin 9054, New Zealand. Fax: +64-3-479 7906; Tel: +64-3-479 7919; E-mail: sbrooker@chemistry.otago.ac.nz*

† Electronic Supplementary Information (ESI) available: Solubility information for the [M^{II}(dpzca)$_2$] complexes, summary of unsuccessful syntheses, additional figures and details of X-ray crystal structure determinations, additional cyclic voltammetry and controlled potential coulometry data, UV-visble spectra and a figure showing the NMR numbering, are available. See DOI: 10.1039/b000000x/

1. M. G. Cowan and S. Brooker, *Coord. Chem. Rev.*, 2012, **256**, 2944-2971.
2. E. I. Lerner and S. J. Lippard, *J. Am. Chem. Soc.*, 1976, **98**, 5397-5398.
3. E. I. Lerner and S. J. Lippard, *Inorg. Chem.*, 1977, **16**, 1546-1551.
4. M. Ferbinteanu, T. Kajiwara, K.-Y. Choi, H. Nojiri, A. Nakamoto, N. Kojima, F. Cimpoesu, Y. Fujimura, S. Takaishi and M. Yamashita, *J. Am. Chem. Soc.*, 2006, **128**, 9008-9009.

5. F. Pointillart, K. Bernot, R. Sessoli and D. Gatteschi, *Chem. Eur. J.*, 2007, **13**, 1602-1609.
6. T. Kajiwara, M. Nakano, Y. Kaneko, S. Takaishi, T. Ito, M. Yamashita, A. Igashira-Kamiyama, H. Nojiri, Y. Ono and N. Kojima, *J. Am. Chem. Soc.*, 2005, **127**, 10150-10151.
7. T. Kajiwara, I. Watanabe, Y. Kaneko, S. Takaishi, M. Enomoto, N. Kojima and M. Yamashita, *J. Am. Chem. Soc.*, 2007, **129**, 12360-12361.
8. S. Zebret, N. Dupont, G. Bernardinelli and J. Hamacek, *Chem. Eur. J.*, 2009, **15**, 3355-3358.
9. A. Kamiyama, T. Noguchi, T. Kajiwara and T. Ito, *Angew. Chem. Int. Ed.*, 2000, **39**, 3130-3132.
10. M. G. Cowan, R. G. Miller, P. D. Southon, J. R. Price, O. Yazaydin, J. R. Lane, C. J. Kepert and S. Brooker, *Inorg. Chem.*, doi.org/10.1021/ic501876m and front cover.
11. M. G. Cowan and S. Brooker, *Dalton Trans.*, 2012, **41**, 1465-1474 and front cover feature.
12. M. G. Cowan, J. Olguín, S. Narayanaswamy, J. L. Tallon and S. Brooker, *J. Am. Chem. Soc.*, 2012, **134**, 2892–2894 and front cover feature.
13. R. G. Miller, S. Narayanaswamy, J. L. Tallon and S. Brooker, *New J. Chem.*, 2014, **38**, 1932-1941.
14. M. Eddaoudi, D. B. Moler, H. Li, B. Chen, T. M. Reineke, M. O'Keefe and O. M. Yaghi, *Acc. Chem. Res.*, 2001, **34**, 319-330.
15. X. T. Li, C. Zhan, Y. Wang and J. Yao, *Chem. Commun.*, 2008, 2444-2446.
16. M. H. Cynamon, S. P. Klemens, T.-S. Chou, R. H. Gimi and J. T. Welch, *J. Med. Chem.*, 1992, **35**, 1212-1215.
17. J. A. King Jr., P. E. Donahue and J. E. Smith, *J. Org. Chem.*, 1988, **53**, 6145-6147.
18. H. Sigel and R. B. Martin, *Chem. Rev.*, 1982, **82**, 385-426.
19. J. M. Rowland, M. M. Olmstead and P. K. Mascharak, *Inorg. Chem.*, 2002, **41**, 2754-2760.
20. H. Kooijman, S. Tanase, E. Bouwman, J. Reedijk and A. L. Spek, *Acta Crystallogr., Sect. C*, 2006, **C62**, m510-m512.
21. R. M. Hellyer, D. S. Larsen and S. Brooker, *Eur. J. Inorg. Chem.*, 2009, 1162–1171.
22. J. Klingele(née Hausmann), B. Moubaraki, K. S. Murray, J. F. Boas and S. Brooker, *Eur. J. Inorg. Chem.*, 2005, 1530-1541.
23. R. Sahu, S. K. Padhi, H. S. Jena and V. Manivannan, *Inorg. Chim. Acta*, 2010, **363**, 1448-1454.
24. T. Inokuma, Y. Hoashi and Y. Takemoto, *J. Am. Chem. Soc.*, 2006, **128**, 9413-9419.
25. A. B. P. Lever, *Studies in Physical and Theoretical Chemistry 33: Inorganic Electronic Spectroscopy*, 2 edn., Elsevier, Amsterdam, 1997.
26. M. G. B. Drew, C. J. Harding, V. McKee, G. G. Morgan and J. Nelson, *J. Chem. Soc., Chem. Commun.*, 1995, 1035-1038.
27. D. J. Tranchemontagne, J. L. Mendoza-Cortés, M. O'Keefe and O. M. Yaghi, *Chem. Soc. Rev.*, 2009, **38**, 1257-1283.
28. J. J. Perry IV, J. A. Perman and M. J. Zaworotko, *Chem. Soc. Rev.*, 2009, **38**, 1400-1417.
29. T. Kajiwara, R. Sensui, T. Noguchi, A. Kamiyama and T. Ito, *Inorg. Chim. Acta*, 2002, **337**, 299-307.
30. V. V. Pavlishchuk and A. W. Addison, *Inorg. Chim. Acta*, 2000, **298**, 97-102.
31. A. L. Spek, *J. Appl. Cryst.*, 2003, **36**, 7-13.
32. P. van der Sluis and A. L. Spek, *Acta Crystallogr., Section A*, 1990, **A46**, 194-201.
33. L. Yang, D. R. Powell and R. P. Houser, *Dalton Trans.*, 2007, 955-964.
34. G. M. Sheldrick, *Acta Crystallogr., Section A*, 1990, **46**, 467-473.
35. G. M. Sheldrick and T. R. Schneider, *Methods in Enzymology*, 1997, **277**, 319-343.
36. G. M. Sheldrick, *Acta Crystallogr., Section A*, 2008, **A64**, 112-122.

TOC Entry

Pyrazine-imide complexes: reversible redox and MOF building blocks

Matthew G. Cowan, Reece G. Miller and Sally Brooker

Stepwise exchange of pyrazine for pyridine, in three bis-heterocycle-based imide ligands, tunes the potential of the $[M^{II/III}(ligand)_2]^{0/+}$ redox couple, increasing the stability of the M^{II} oxidation state by about 0.1 V per exchange.